Challenges in Applying Surface Analysis Methods to Nanoparticles and Nanostructured Materials

D.R. Baer[*], M. H. Engelhard, D. J. Gaspar, D. W. Matson, K. H. Pecher, J. R. Williams, and C. M. Wang

Pacific Northwest National Laboratory, PO Box 999, Richland, WA 99352, USA

*don.baer@pnl.gov

Nanostructured materials of various types and forms are formulated in a variety of novel ways and have been increasingly subjected to many types of chemical and physical analysis. Since nanomaterial systems contain a relatively large amount of surface or interface area, it should be natural to characterize them using tools designed to analyze such surfaces and interfaces. We have found that nanoparticles and other nanostructured materials present a variety of analytical challenges. This paper reviews environmental effects on measurements of Ce-oxide nanoparticles and nanoporous silica films and focuses on efforts to quantify the ion damage and sputter rates for the Fe-oxide nanoparticles. We have found that nanoparticles appear more readily damaged and to have sputter rates that exceed those of the corresponding "bulk" materials. To verify such effects, we need to know many details about the nanoparticle size, size distribution, density, shape and history that are not always easily obtained.

INTRODUCTION

Nanoscience and nanotechnology are near the forefront of exciting areas of science and technology and as a result, a significant amount of the world's resources available for research are focused in areas broadly classified as "nano" in some fashion [1]. The availability of new generations of analysis tools has played a significant role in making this "nanorevolution" possible. Although the scanning probe microscope may be the single greatest advance in the area of nanomaterials characterization, scanning and transmission electron microscopes, near field optical imaging, synchrotron based x-ray measurements and surface sensitive analysis methods all have had some impact.

Upon reading many papers about nanostructured materials, readers may be left with the impression that these materials are rather ideal in a way that other materials we commonly examine with surface analysis tools are not. Many reports discuss the properties of nanostructured Au, Ag, ZnO, CdSe and other materials as if they were ideal systems existing in a vacuum. Often these materials have been produced and measured either in air or in a liquid, and the surface reactions and contamination that impact most materials are present, but are not discussed. Since many nanostructured materials are comprised mostly of surfaces, the low level of attention paid to surface issues can become a concern. Two specific examples for which surface properties of nanomaterials have been considered serve to highlight the importance of this issue. Prof. Banfield's group [2] has observed that the structure of ZnS nanoparticles depends upon the nature of the environment. Although this is not totally unexpected based on what is known about surfaces and interfaces, many people are surprised by the idea that for nano-sized objects the internal structure of nanoparticles may depend on what is attached to their surfaces. Work by Prof. Gamelin's group on doped ZnO particles [3] shows the importance of composition on different properties of nanoparticles. They grow their particles in solutions doped with Co or other magnetic transitions metals and have made several interesting observations. Specifically, they cannot dope particles formed in solution when the

particles are below a critical size. When the particles grow to a size large enough to allow doping, the optical properties of the particles depend on the location of the Co: surface Co has a different impact than Co in the interior of the nano particles. Furthermore, when the particles cluster their optical and magnetic properties again change. Thus, the properties of the particles can be altered by what is on the surface, as well as whether the particles are loosely aggregated or isolated.

At least in some cases surface adsorbates, contamination or component segregation may alter the behavior and properties of nano-sized objects. Surface analysis methods have been developed to address these issues. Although there are exceptions [4] most often these analytical methods are readily applied to flat films or materials that are treated as flat surfaces, even if they are not. Metrology of nanostructured materials is one of the grand challenges being considered by the United State National Nanoscience Initiative. At a workshop held in January 2004 it was noted that there are significant challenges in obtaining the desired information about any specific nanoparticle, and a significant need exists for methods to collect relevant data about the quality and property distribution of large collections of nano-objects [5].

Because of the wide variety of nanoscience and nanotechnology research projects, there is an increasing need to analyze specimens that have nano features of some type. In our laboratory we are finding that the analysis of these structures presents a variety of challenges. In some cases, the challenges relate to an understanding of new and unexpected properties of the materials present in the nano-size regime. In other cases, the high surface area of nano-structured materials amplifies what in the analysis of films or bulk materials may be viewed as small or even trivial issues.

It is common practice to rinse many types of specimens with a solvent, including alcohols such as isopropyl alcohol (IPA) before inserting them into vacuum for surface analysis. During studies of nano-porous silica films, we found that such a rinse altered the depth profiles of these films as shown in Fig. 1. The apparent film thickness was approximately 25% thicker after an IPA rinse compared to unrinsed samples. IR spectroscopy and other measurements suggest that the rinse is removing materials from within the film and that some IPA is retained [6]. Although IPA normally has adequate vapor pressure to be readily removed in vacuum, evidence suggests that at least some of the IPA remains in the film during normal pump down and analysis times in vacuum causing an apparent increase in film thickness upon sputtering [6].

Another area of importance for many nanostructures is their stability as a function of time and environment. Changes in ZnS nanoparticles as the environment was altered have been already noted. There are many studies of nanostructured CeO_2 because of the importance of this material to catalysis and as a component for fuel cell electrodes [7,8]. Several have observed that the lattice parameter and oxidation state change as CeO_x particles decrease in size. In particular, as observed by TEM and energy loss spectra, there is a tendency for the formation of Ce^{+3} with decreasing particle size[8]. We have measured a difference of oxidation state for 3 nm nanoparticles relative to thin film material, as shown in Fig. 2. We found the somewhat disturbing trend that the extent of the Ce^{+3} in 3 nm nanoparticles varies with time while XPS measurements are being collected. In contrast, a CeO_2 thin film (Fig. 2b) shows very little damage and very little Ce^{+3}. The earlier results [8] suggest that ceria nanoparticles are unstable against the formation of lower oxidation state defects. Although equilibrium defect concentration may depend upon particle size and temperature, the addition of energy from other sources such as X-rays and the resulting electron cascades appears to alter the oxidation state of the particles raising a general concern about the impact of probing beams on the measured properties of nanoparticles.

Our questions about nanoparticle stability and surface measurements were initiated by work on Fe nanoparticles. We have been growing metal and oxide Fe nanoparticles and measuring their chemical properties [9] using a variety of methods. In several cases the particles are observed to have a structure consisting of a metallic core surrounded by an oxide
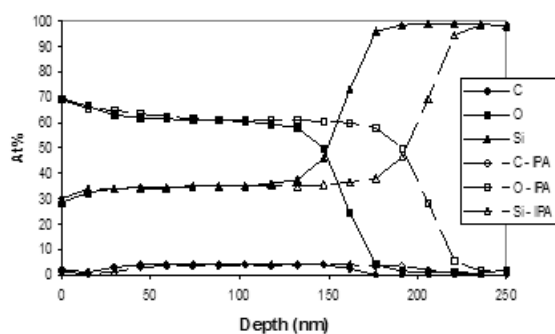
Fig. 1 Apparent thickness change in sputtering of plasma processed nanoporous SiO_2 film with and without rinsing in IPA. When compared to SiO_2 films of known thickness, the samples with no IPA exposure is 157 nm thick and the sample with IPA exposure is 204 nm thick.
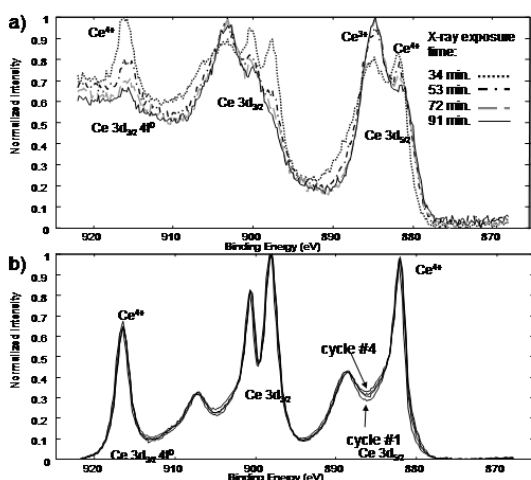

Fig. 2 a) 3d photoelectron spectra of 3nm ceria particles as examined in a Phi Quantum 2000. Note that the amount of Ce3+ increases with x-ray exposure. b) Very little Ce3+is found in the thin film, although some very small amount of damage may occur with prolonged x-ray exposure.

shell while in other cases the particles are completely oxide. Initial measurements have suggested that Fe-oxide nanoparticles may be more susceptible to damage in an ion beam than films and that they may sputter faster than similar 2-dimensional oxide films. The remaining portions of this paper summarize our efforts to determine if Fe-oxide nanoparticles are more easily damaged and if the sputter rates are

different from those of films having a similar composition. Initial indications of possible enhanced damage during analysis of nanoparticles were observed on a few types of material, and the experiments to be described were our attempt to more carefully examine the phenomena. Attention in this work is focused on one set of nanomaterials and our efforts to gather information needed to answer the questions. Although the results obtained are not fully definitive, they nicely highlight the challenges involved and describe the approaches needed.

Experimental

Iron – Oxide Nanoparticles –

The nanoparticulate material studied in this paper was produced in a linear laminar flow reactor by UV irradiation of iron pentacarbonyl (IPC) entrained in nitrogen gas by bubbling nitrogen through liquid IPC. The entrained precursor was injected into a quartz reactor tube (1/2" OD by 3.5" long) through a length of 1/16" stainless steel tubing mounted in one leg of a Swagelok tee connected to one end of the reactor. Additional nitrogen was introduced as a sheath gas through the third leg of the tee. The flowing entrained precursor was exposed to UV irradiation from a Spectral Energy UV source to remove carbonyl groups and nucleate solid particle growth. The nanoparticulate product was collected electrostatically by flowing the nitrogen sheath gas and suspended product particles through a grounded wire mesh and past a ~8mm square Au-coated silicon wafer chip to which a 36 KV DC voltage was applied. Material was collected for a period of 1 minute. Collection was performed in a special glass enclosure that could be sealed for transport of the product in an anaerobic nitrogen atmosphere prior to analysis.

For comparison purposes a 17 nm thick Fe_2O_3 oxide film was grown by Oxygen Plasma Assisted - Molecular Beam Epitaxy (OPA-MBE) on a chromia layer deposited on a sapphire substrate. This system has been previously reported and is well characterized [10]. The composition of the film was verified by X-ray photoelectron spectroscopy (XPS), the structure by X-ray diffraction (XRD) and the thickness was verified by X-ray reflectivity measurements. This film was sputter profiled by a 2 kV Ar ion beam rastered over a 4 mm by 4 mm area,
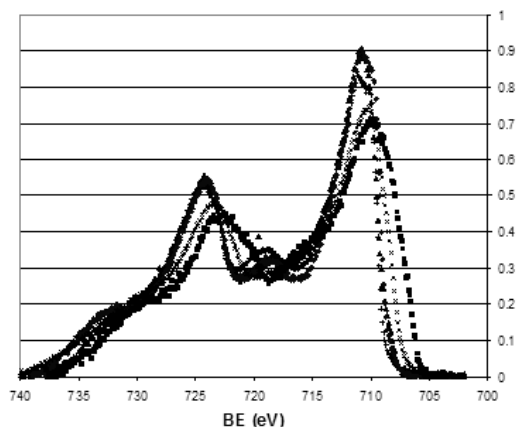
Fig 3. Fe 2p x-ray photoelectron spectra of iron films and 3 nm nanoparticles before ion bombardment and after ion bombardment. Although there are some slight differences data from Fe_2O_3 films 1(+) and 2( ) are nearly the same as the nanoparticle (▲). However after the particle sputtering an equivalent of 0.4 nm, the particles (■) appear much more damaged that the film after sputtering 0.66 nm (x).

producing a sputter rate of 5.7 Å/min. For identical conditions the sputter rate for a SiO_2 film was 8.7 Å/min, or ~1.5x the removal rate of the Fe_2O_3 film.

Electron Microscopy - High-resolution TEM was performed using a Jeol JEM 2010 operated at 200 kV. All images were digitally recorded using slow scan 1024 x 1024 CCD cameras and processed using Digital Micrograph (Gatan). The specimen was collected by transferring a small amount of material from the Au-coated substrate to a TEM grid. The samples were exposed to air for a short period of time as they were introduced into the microscope.

X-ray Photoelectron Spectroscopy - As described above, nanoparticulate samples collected for XPS analysis were deposited on an Au-coated Si substrate in the laminar flow reactor. They were removed from the deposition system in the sealed container and placed in a glove box before XPS analysis, and were subsequently transferred to the XPS entry chamber through a nitrogen glove bag. The XPS measurements were performed using a Physical Electronics Quantum 2000 Scanning ESCA Microprobe with a focused monochromatic Al Kα X-ray (1486.7 eV) excitation source, a spherical section analyzer and a 16-element multichannel detection system. The X-ray beam was a 105 W, 100 μm X-ray beam spot scanned over a 1.4

mm x 0.2 mm rectangle on the Au-coated sample substrate. The X-ray beam was incident normal to the sample and the X-ray photoelectron detector was at 45° off normal. Data was collected using a pass-energy of 23.5 eV. For the Ag 3d5/2 line, these conditions produced a FWHM of 0.77 eV. The binding energy (BE) scale was calibrated using the Cu 2p3/2 feature at 932.62 ± 0.05 eV and Au 4f at 83.96 ± 0.05 eV for known standards. To minimize charging of the samples, 1 eV, 20 uA electrons and low energy Ar^+ ions were used for analysis. Ion sputtering was conducted using 2kV Ar^+ ions rastered over a 4 mm x 4 mm area. The sputter rate for the Fe_2O_3 was determined using the known sample thickness and was compared to the rate for SiO_2 layers on silica that we normally use for a sputter rate reference.

RESULTS AND DISCUSSION
Nano-particle chemical state and structure –

The small quantity of nanoparticulate material deposited on the Au did not allow XRD analysis of structure or composition. TEM analysis indicated that the deposit was made up of primary particles of ~ 5 nm as revealed by dark field imaging. On the TEM grid after tranfer from the Au-coated Si they were somewhat aggregated, with some of the aggregates appearing as up to 20 nm wide strands of material. Since there was a post-collection transfer of material from the Au-coated substrate to the TEM grid, the aggregation may or may not have been representative of the as-deposited particles. The size of the particles and any aggregate is an important input to understanding the XPS data and a limitation of the understanding of the current results. The TEM did not observe a core-shell structure, but provided indication that all the material was oxidized. This is consistent with Fe L-edge X-ray adsorption measurements which showed a predominant +3 oxidation state of similar materials deposited on Si_3N_4 wafers.

XPS data from the raw particles matched quite well two different versions of Fe_2O_3 Oxygen Plasma Assisted-Molecular Beam Epitaxy OPA-MBE films (Fig. 3). Based on the TEM indication that the particles were all oxide with no core-shell structure, the results support the views that the particles were a nanoparticle version of Fe_2O_3 with particle size of

approximately 5 nm. Although the measurements were not done on this specific batch of material, additional nano-particles deposited in the same fashion were examined by X-ray diffraction, X-ray adsorption, electrochemical studies and other analysis methods as described in ref. 9 and only indication of the fully oxidized state of Fe was found. We therefore conclude that the 5 nm particles discussed in this paper were fully oxidized Fe; Fe_2O_3 with most likely some FeOOH or similar hydroxide species on the surface.

Damage and Sputter Rate – Changes in the Fe 2p photoelectron peaks produced by small amounts of 2 kV Ar ion sputtering of the nanoparticles and thin film of Fe_2O_3 are also shown in Fig. 3. For a smaller amount of sputtering a greater change is observed for the nanoparticles than for the film. The Au, O, C and Fe signals converted to atomic % are shown in Fig. 4 as a function of the amount of sputtering (referenced to the sputter rate for the Fe_2O_3 film). When less than one nm of material was removed from the film, the Fe signal from the particles was reduced by 50%.

It is rather easy to argue that we might expect nanoparticles to damage more easily and that the sputter rate might be considerably higher for the small particles than for a thin film. Possible arguments to account for easy damage and rapid sputtering include the similarity of particle size to the size of an ion collision cascade, observed instability of nanoparticles such as observed for CeO_2 and the simple fact that particles have a large amount of surface area from

Fig 5. Schematic drawing showing assumed distribution of damage layer on film (a) and particles (b). To model the signals to be expected, the damaged particles are assumed to be made up of concentric multi-layered cylinders (c) oriented in the direction of the analyzer. Each cylinder can be considered a thin film structure from the point of view of electron emission and the signal intensities readily calculated.

which sputter products can emerge.

However, roughly spherical nanoparticles have a significantly different shape than a flat film and it is appropriate to ask what the signals from nanoparticles damaged uniformly on the surface might look like. As noted in ref. 4, the signals from an outer layer on a curved spherical or cylindrical substrate are enhanced relative to the substrate signals that would be observed for the same overlayer on a flat substrate. Therefore, we set out to learn what information was needed to determine if nanoparticles were actually damaged more readily than the thin film and if the sputter rate was significantly different for the particles relative to a film.

Fig. 6 Fraction of measured signal attributed to the Fe^{+2} or damage basis spectrum for sputtered nanoparticles and Fe_2O_3 film. The sputter depth indicated is based on the sputter rate for the Fe_2O_3 film.
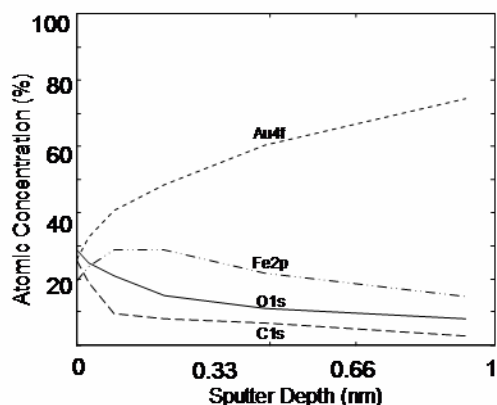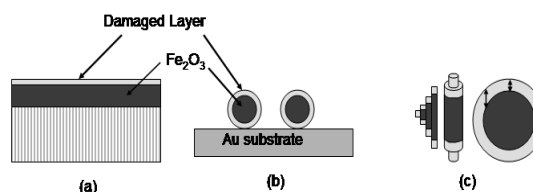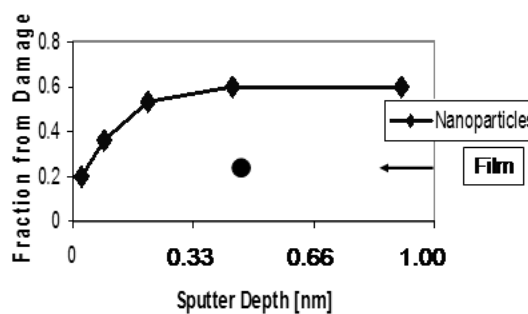

Fig. 4 Sputter profile of nanoparticles using conditions described in the text. The sputter rate was that determined from the thin film. Ion sputtering that would remove less than 1 nm of material for a bulk film removes 50% of material in 5 nm particles.

As one effort to determine if the Fe-oxide nanoparticles were actually altered to a greater extent than the film during sputtering, we assumed the damage that was produced in a thin layer of the film occurred on the whole surface surrounding the

nanoparticles (Fig. 5 a and b). Assuming that we have reasonable information about electron escape depths and particle size and shape (we assumed a spherical shape and 5 nm particle size) it is possible to determine the relative amounts of signal that would be observed from damaged vs. undamaged layers of a particular thickness on both a flat film and nanoparticles of a particular size.

Comparing the damage extent between the film and particles requires either an absolute or relative measurement of the extent of damage for each. Quantitative estimates of the damage to the particles and the film were based on the ratio of damaged (Fe^{+2} basis or reference spectra) and undamaged (Fe^{+3} reference or basis spectra) needed to approximately fit the Fe 2p XPS peaks for the sputtered films and sputtered nanoparticles. It was assumed that part of the signal from each sample was the Fe^{+3} curve of the undamaged particles (Fe^{+3} basis spectrum) and that the second portion of the signal was due a damage-induced Fe^{+2}. Although different approaches were used to estimate the shape of the Fe^{+2} damage basis spectrum, no approach was entirely satisfactory. The shape of the Fe^{+2} obtained from combining the Fe^{+3} basis spectrum and Fe_3O_4 data produced an Fe^{+2} spectrum in the appropriate ratio and was qualitatively similar to a difference spectrum obtained by substracting a fraction of the normalized Fe^{+3} basis spectrum from the most damaged particle. However, the ideal crystal of Fe_3O_4 and the damaged nanoparticles (and film) produced different peak
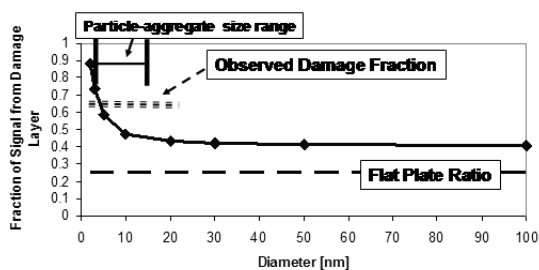

Fig. 7 Comparison of the calculated fraction of signal from the damage layer to that observed in the iron nanoparticles. The thickness of the damage layer (0.5 nm) used in the model was adjusted so that the fraction of damage signal for the flat plate was equal to what is observed for the sputtered thin film from Fig. 6. Assuming 5 nm particles, the model indicates that the damage layer on the particles is approximately the same as that observed for the film.

widths for the Fe^{+2} damage spectrum. The damaged particle peak required a broader Fe^{+2} damage spectrum (for both the film and especially the particle), possibly indicating the significant disorder associated with sputter damage. The most consistent fits were obtained using a Fe^{+2} basis inferred from the damaged particles. The results of fitting the assumed basis spectra to both the film and particle data has no valid claim to absolute accuracy; although it should provide a self consistent indication of the relative amounts of the two types of spectra needed to produce the measured signals. The fraction of the total iron signal attributed to damage (Fe^{+2}) is shown in Fig. 6 as a function of sputter dose.

The "layers on a plane" model is described in ref 4 and in several other locations, including by Martin Seah [11]. This model was used to calculate the XPS signals from layered structures. The inelastic electron for both damaged and undamaged oxides based on IMFP values obtained using QUASES-IMFP-P2M [12] inelastic electron mean free path calculation that uses the Tanuma, Powell, and Penn algorithm TPP2M [13]. Our implementation of the flat plate model to spheres involved breaking the spheres into 2000 concentric cylinders (Fig. 5 c) and applying the flat plane model to each cylindere. Although qualitatively the results do not change with increasing the number of cylinders, it was possible to analytically calculate the ratio of the volumes of the shell and core of the nanoparticles and compare that to the sum of cylinders. The larger number of cylinders was used to assure agreement of the volumes of material in the damage coating and "core" of the nanoparticles.

In connecting the data from Fig. 6 to the model calculations as shown in Fig. 7, the thickness of the damage layer for the thin film was adjusted so that approximately 27% of the signal from the flat film arose from the damaged layer. It is useful to remember that for the sphere the electrons traveled along the axis of the cylinder to the analyzer while for the film the angle between the surface normal of the film and the analyzer was 45 degrees.

A few observations immediately follow from the figure. First, the damaged to undamged signal ratio for any sphere is larger than the corresponding ratio from a flat plate. Second, as the particle size

decreases, the relative amount of damage signal increases. Third, for 5 nm particles, the amount of damage observed is approximately what would be expected if the particles were actually 5 nm spheres and the damage layer surrounding all of the sphere was the same as the flat plate. Thus, assuming that 5 nm is appropriate size of the particles, there is little evidence that these particular nanoparticles are actually damaged to a significantly different extent than the film. However, if the relevant particle size were really the 10 to 20 nm aggrogates observed by the TEM, there was more damage than would be expected.

Determining the sputter rate for nanoparticles may also be a challenge, even in concept. However, it may not be unreasonable to consider the mass of the nanoparticles and the thickness that would be expected if the spheres were reconfigured into a uniform thin film. The 5 nm particles would pack into a film of approximately 2.5 nm thickness. The data in Fig. 4 indicates that less than 1 nm of film sputtering removes half of the nanoparticle intensity, or a little less than half of the material equivalent for a 2.5 nm film. With these assumptions, the apparent sputter rate of the nanoparticles is somewhat higher than that of the thin film, but any enhancement for the particles did not appear to be large. However, as suggested for the damage observed above, this conclusion would be altered if the relevant particle size was actually the 10 or 20 nm aggregates observed in the TEM measurements. If the relevant characteristic size is actually 10 or 20 nm, the effective rate of sputtering for the nanoparticles would be significantly greater than for a film.

For the iron nanoparticles examined here, assuming that "primary" particle size to be 5 nm as indicated in the TEM, at least most part of the apparent enhanced amount of damage and apparent increased rate of sputtering were associated with the size and shape of the materials and do not clearly represent a significant deviation of the particle properties from the behaviors of the thin film. Accurate determination of these rates and understanding of their implications requires both knowledge obtained form other methods and application of detailed modelling. A more accurate understanding of the effects of TEM sampling and mounting of material for surface spectroscopy is needed to fully quantify these effects.

SUMMARY

We conclude that because of size and shape effects, the interactions of nanoparticles and nanostructured materials with their environments can impact their measured properties in a variety of ways. Understanding the meaning of nanoparticle measurements may frequently require combining information from a variety of techniques. Unexpected results of many types may be observed, and detailed consideration of the experimental results as well as modeling of the data may be needed to understand the true meaning of the measurements.

Nano-structured materials will be subject to the same impurity and contamination issues that make surface analysis methods useful in many circumstances. However, the useful application of those methods to nano-structured materials requires addressing a new set of analysis issues.

ACKNOWLEDGEMENTS

REFERENCES

[1] D. R. Baer, P. E. Burrows and A. A. El-Azab, *Progress in Organic Coatings* **47**, 342 (2003).

[2] H. Zhang, B. Gilbert, F. Huang & J. F. Banfield, *Nature* **424**, 1025 (2003).

[3] D. A. Schwartz, N. S. Norberg, Q. P. Nguyen, J. M. Parker, and D. R. Gamelin, *J. AM. CHEM. SOC.* 125, 13205 (2003).

[4] For example see XPS multiquant, a computer code developed by Miklos Mohai of the Hungarian Academy of Sciences to deal with particles, rods and other structures that make up

the surface being analyzed.
(http://www.chemres.hu/AKKL/XMQpages/XMQ home.htm)

[5] NNI Interagency Workshop, Instrumentation and Metrology for Nanotechnology Grand Challenge Workshop https://metrology.nano.gov

[6] D. J. Gaspar, M. H. Engelhard, M. C. Henry and D. R. Baer, "Real and Apparent Erosion rate variations during XPS sputter depth profiling of nanoporous films" *Surface and Interface Analysis* **37**, 417 (2005).

[7] M. A. Henderson , C. L. Perkins, M. H. Engelhard, S. Thevuthasan, and C. H. F. Peden, *Surface Science* **526**, 1 (2003).

[8] L. Wu H. J. Widemann, A. R. Moodenbaugh, R. F. Klie, Y. Zhu, D. O Welch and M. Suenaga,   *Phys. Rev.* **B69**, 125415 (2004).

[9] J. T. Nurmi, P. G. Tratnyek, V. Sarathy, D. R. Baer, J. E. Amonette, K. Pecher, C. Wang, J. C. Linehan, D. W. Matson, R. L. Penn, and M. D. Driessen, Characterization and Properties of Metallic Iron Nanoparticles: Spectroscopy, Electrochemistry, and Kinetics, *Env. Sci. Technol.* **39**, 1221 (2005).

[10] S.A. Chambers, Y. Liang, Y. Gao, *Phys. Rev.* **B61**, 13223 (2000).

[11] Martin Seah "Quantification of AES and XPS" chapter 5 in *Practical Surface Analysis Volume 1- Auger and X-ray Photoelectron Spectroscopy* second edition edited by D. Briggs and M. Seah John Wiles and Sons, Chichester (1990).

[12]QUASES-IMFP-TPP2M™, Software Package - Ver.2.1, Developed by S. Tougaard available free to download at http://www.quases.com/

[13] S. Tanuma, C. J. Powell, D. R. Penn, *Surface Interface Analysis,* **21**, 164 (1993).